

*promoting access to White Rose research papers*



**Universities of Leeds, Sheffield and York**  
**<http://eprints.whiterose.ac.uk/>**

---

This is an author produced version of a paper published in **Physical Review B**.

White Rose Research Online URL for this paper:

<http://eprints.whiterose.ac.uk/74889>

---

**Published paper**

Chen H.R., Freeman, C.L., Harding, J.H. (2011) *Charge disproportionation and Jahn-Teller distortion in LiNiO<sub>2</sub> and NaNiO<sub>2</sub>: A density functional theory study*, Physical Review B, 84 (8), Article number: 085108

<http://dx.doi.org/%2010.1103/PhysRevB.84.085108>

---

# Charge disproportionation in LiNiO<sub>2</sub>? – A Density Functional Theory Study

H. Chen, C. L. Freeman and J.H. Harding

Department of Materials Science and Engineering, University of Sheffield, S1 3JD, United Kingdom

## Abstract

Density functional theory calculations have been performed on three potential ground-state configurations of LiNiO<sub>2</sub> and NaNiO<sub>2</sub>. These calculations show that, whereas NaNiO<sub>2</sub> shows the expected cooperative Jahn-Teller distortion (and therefore a crystal structure with  $C2/m$  symmetry), LiNiO<sub>2</sub> shows at least two possible crystal structures very close in energy (within 3 meV/f.u.):  $P2_1/c$  and  $P2/c$ . Moreover, one of them ( $P2/c$ ) shows charge disproportionation of the (expected) Ni<sup>3+</sup> cations into Ni<sup>2+</sup> and Ni<sup>4+</sup>. We discuss the implications of this complex ground state for the interpretation of the available electron and neutron structure data, its electronic and complex magnetic behaviour.

## Introduction

LiNiO<sub>2</sub> has attracted considerable interest due to its potential application as a cathode material in lithium ion batteries. Although this compound has been intensively studied for many years, the local geometry, electronic and magnetic structure are still highly debatable. The analysis of the data is complicated by the well-known difficulty of synthesising truly stoichiometric LiNiO<sub>2</sub>. Experimentally, both Ni<sup>2+</sup> and Ni<sup>3+</sup> in LiNiO<sub>2</sub> have been reported using various detection techniques<sup>1-4</sup>. Even the most recent experimental studies struggle to obtain truly stoichiometric material. Where quoted, typical defect concentrations are of the order of a few percent – nickel is found on the lithium site of the perfect structure<sup>5</sup>.

Unlike the analogous sodium compound, NaNiO<sub>2</sub>, LiNiO<sub>2</sub> shows neither long-range magnetic disorder nor a long-range cooperative Jahn Teller effect despite the fact that all calculations until now (for example<sup>6,7</sup>) in LiNiO<sub>2</sub> show that Ni is present as low-spin Ni<sup>3+</sup> with an electronic configuration  $t_{2g}^6 e_g^1$  which is Jahn-Teller active. Two different Ni-O bond lengths have been observed both in EXAFS<sup>8,9</sup> and neutron diffraction<sup>5</sup> which are attributed to a *local* Jahn-Teller distortion, unlike the cooperative distortion seen in other Jahn-Teller active systems such as NaNiO<sub>2</sub> and LiMnO<sub>2</sub>. The analysis of the neutron partial density function (PDF) in [5] supports the hypothesis of a Jahn-Teller distortion since their results show four bond-lengths grouped as “long bonds” (2.04 Å and 2.06 Å with an average length of 2.05 Å) and “short bonds” (1.90 Å and 1.96 Å with an average length of 1.93 Å) suggestive of the 2:1 ratio of short to long bonds expected for Jahn-Teller distortion. However, the long-range PDF peaks increase in height with temperature – an unusual effect that the authors attribute to domain formation.

The magnetic properties of LiNiO<sub>2</sub> have been a matter of debate since the first measurements in 1958<sup>10</sup>. Reynard *et al*<sup>11</sup> suggested, on the basis of anomalies in the spin susceptibility observed at 10 K and 400 K, that there were at least two energy scales

involved, corresponding to spin and orbital interactions, and that the possibility of orbital frustration should be considered. The neutron studies of [5] argue against this since this would imply that the number of “short” and “long” Ni—O bonds would be equal. The authors suggest instead that the magnetic properties should be explained by the assumption that there is local orbital ordering: the  $3d_{z^2-r^2/3}$  orbitals of three  $\text{Ni}^{3+}$  ions point towards their shared oxygen. This model also receives support from a recent electron diffraction study<sup>12</sup>. However, there remain problems with the interpretation of the magnetic data using this scheme; in particular the coexistence of ferromagnetic and antiferromagnetic spin fluctuations. It is argued<sup>5</sup> that the existence of domains, required to prevent stress buildup caused by the trimer ordering, may restrict the antiferromagnetic fluctuations. A recent set of first principles density functional theory (DFT+U) calculations has been performed on the possible local orderings for Jahn-Teller distortions in  $\text{LiNiO}_2$ <sup>13</sup>.

A whole range of possible electronic ground states are possible in compounds that have a nominal  $\text{Ni}^{3+}$  charge state, from a totally delocalized metal ( $\text{LaNiO}_3$ ) to a strongly localized orbital ordering insulator ( $\text{NaNiO}_2$ ). This is shown in Table 1 where the behaviour is correlated with the nickel-oxygen bond length ( $d_{\text{NiO}}$ )

**Table 1:** The Ni-O bond lengths ( $d_{\text{Ni-O}}$ ) in compounds with the nominal valence state  $\text{Ni}^{3+}$  compounds and their ground state behaviour. Numbers of Ni-O bonds of a given length given in brackets. \* Note that the Ni-O bond lengths differ between studies of  $\text{LiNiO}_2$

Compound	$d_{\text{Ni-O}}$ (Å)	$\langle d_{\text{Ni-O}} \rangle$ (Å)	Electronic ground state
$\text{LaNiO}_3$ <sup>14</sup>	1.93 [6]	1.93	Metallic (delocalised)
$\text{NdNiO}_3$ <sup>15</sup>	1.93[2], 1.94[2], 1.96[2]	1.94	Charge ordering insulator
$\text{LuNiO}_3$ <sup>16</sup>	1.89[2], 1.92[2], 1.94[2] 1.97[2], 2.00[2], 2.02[2]	1.96	Charge ordering insulator
$\text{YNiO}_3$ <sup>17</sup>	1.90[2], 1.92[2], 1.94[2] 1.96[2], 2.01[2], 2.01[2]	1.96	Charge ordering insulator
$\text{AgNiO}_2$ <sup>18</sup>	1.95 [6]	1.95	Moderately charge ordering, $3\text{Ni}^{3+} \rightarrow \text{Ni}^{2+} + 2\text{Ni}^{3.5+}$
$\text{LiNiO}_2$ <sup>5</sup>	1.90[4], 1.96[4], 2.04[2], 2.06[2]	1.97*	
$\text{NaNiO}_2$ <sup>19</sup>	1.92[4], 2.15[2]	2.00	Orbital ordering insulator

Charge disproportionation is also reported for other rare earth nickelates<sup>20</sup>. It can be seen from the above table that in the case of  $\text{LiNiO}_2$  there is could be a competition between charge ordering and orbital ordering for the ground state. The purpose of this paper is to demonstrate that this is indeed the case using first principles density functional theory and to discuss the consequences.

## Theoretical Methods

$\text{LiNiO}_2$  is frequently reported to crystallise in the hexagonal structure with  $R\bar{3}m$  space group symmetry. A slight monoclinic distortion was observed at low temperatures (10 K) by the

neutron diffraction study of [5] and a better fit found to the  $C2/m$  space group, but detailed analysis showed that the collinear ordering of the Jahn-Teller distortions implied by this space group was not supported by a combination of the Rietveld refinement and the neutron PDF data. The electron diffraction study of [12] was analysed using the  $Pm$  space group (which is the simplest space group that can incorporate a trimer ordering model).

A considerable amount of work has been done on both lithium-doped NiO and  $\text{LiNiO}_2$  (which can be viewed as a special case of lithium doped NiO where the doping level is 50% and the Li and Ni positions are ordered on the (111) planes. Calculations on lithium-doped NiO have argued that the hole is localised on the oxygen ion<sup>21,22</sup>, a position supported by the interpretation of oxygen K-edge X-ray absorption spectra<sup>23</sup>. However, the considerable volume of calculations on  $\text{LiNiO}_2$  is united in interpreting this compound as contained  $\text{Ni}^{3+}$  (see, for example [6,7,13,24-25]). This is reinforced by the extensive magnetic data now available<sup>11,26</sup>. None of this denies that there is considerable charge transfer between the nickel and oxygen, but it does assert that interpretations in terms of holes on the nickel ions make better sense of the data for  $\text{LiNiO}_2$ . The two interpretations are not unconnected, as Anisimov *et al*<sup>27</sup> point out.

Previous density functional calculations<sup>13,25</sup> have predicted that distortions with  $C2/m$  symmetry lower the cohesive energy but did not consider charge disproportionation. In order to investigate the various possible electronic relaxations in  $\text{LiNiO}_2$  we have used four unit cells as starting configurations. Two of these,  $R\bar{3}m$  and  $C2/m$  cells (each with one formula unit) have been discussed before. In addition, two more cells are proposed and discussed below. One cell contains a zig-zag Jahn-Teller orbital ordering of the  $\text{Ni}^{3+}$  ions (also discussed in [5 and 13]) and has  $P2_1/c$  symmetry with two formula units. The other cell, with  $P2/c$  symmetry containing four formula units, but retaining good agreement with the measured lattice parameters of the low temperature structure, was constructed for the charge disproportionation model. As far as we are aware, no attempt has been made to analyse the experimental data using the  $P2/c$  space group. We have also investigated the  $Pm$  unit cell suggested by Cao *et al*<sup>12</sup> (8 formula units) but, as we shall show, when the cell geometry is optimised, it becomes indistinguishable from  $C2/m$ .

First-principles DFT calculations using the generalised gradient approximation (GGA) and the Perdew, Burke and Ernzerhof (PBE) functional<sup>28</sup> were performed using the projector-augmented wave (PAW)<sup>29</sup> method to investigate the ground state crystal and electronic structure of  $\text{LiNiO}_2$ . It has been shown previously<sup>30</sup> that the simpler Local Density Approximation cannot give the Jahn-Teller distortion. It is also well known that the GGA functional does not give the correct electronic description of strongly correlated systems such as transition metal oxides. One possible solution is to perform calculations with full exchange. However this requires large amounts of computer resources and is impractical for the size and number of calculations we need to perform. We have, however, performed a

hybrid exchange calculation on the highest symmetry ( $R\bar{3}m$ ) cell as a check on the simpler method we intend to use.

This approximation, known to work well for these systems, is to include an on-site coulomb interaction, the Hubbard  $U$  parameter, in the standard DFT calculations, known as the DFT+ $U$  method<sup>27,31</sup>. The rotational invariant form<sup>31</sup> of the DFT+ $U$  formalism was used and  $U_{\text{eff}} = U - J$ , the onsite correction, was set to be 6.5eV for Ni 3d electrons. This was based on values obtained from a self-consistent calculation<sup>32</sup>. Other work<sup>13</sup> has used a smaller value of  $U_{\text{eff}}$ . The reference gives no justification for this number and we presume it was chosen to produce a reasonable band-gap. For this reason we prefer the higher value. It is, however, important to demonstrate that results of calculations are not strongly dependent on the value of the  $U_{\text{eff}}$  parameter chosen and we provide evidence for this below. The inclusion of the  $U$  parameter has been shown to successfully reproduce the charge disproportionation in  $\text{LiMn}_2\text{O}_4$ ,  $\text{LuNiO}_3$ ,  $\text{NdNiO}_3$ ,  $\text{YNiO}_3$  and used to investigate possible charge-orbital orderings in  $\text{Fe}_3\text{O}_4$ <sup>18, 33-36</sup>. The cut off energy for plane-waves was set at 500 eV. For all cells, the k-point spacing is less than  $0.03 \text{ \AA}^{-1}$  in the Brillouin zone. Convergence of the energy was confirmed for both these parameters. For geometry optimisation, the force was converged to less than  $0.01\text{eV \AA}^{-1}$  per ion. In all cases, the cells were fully optimised assuming the starting symmetry of the cell. All calculations were carried out using the Vienna *ab initio* simulation package (VASP)<sup>37</sup>.

## Results and Discussion

We have calculated the structures and lattice energies of the four unit cells discussed above and present our results both for the structure and relative energies of the cells (using the  $R\bar{3}m$  cell as a baseline for convenience). The relative ordering of lattice energies for the four cases is independent of the choice of the  $U_{\text{eff}}$  value provided that value falls in the range 5.5-7.0eV as shown in Figure 1. Outside this range, the  $P2/c$  is destabilised relative to the  $C2/m$  and  $P2_1/c$  cells. Previous work<sup>13</sup> using a smaller value of  $U_{\text{eff}}$  (4.5eV) is still comparable since, as can be seen from Figure 1, the relative energies of the  $C2/m$  and  $P2_1/c$  cells change little over a very wide range of  $U_{\text{eff}}$  values. Even for a value of  $U_{\text{eff}}$  as low as 4.5eV, the  $P2/c$  cell is comparable in energy with the  $C2/m$  and  $P2_1/c$  cells. We note comparison with previous work where relevant (and consider only the fully relaxed cases) but our aim is rather different to theirs since we wish to consider whether the charge disproportionation cell can be lower than any Jahn-Teller ordering. Structural data for the cells is given in Table 1 for the chosen  $U_{\text{eff}}$  value of 6.5eV. All further results use this value. It is convenient to consider the results for the unit cells in turn.

**Figure 1:** Stabilisation energies (relative to the  $R\bar{3}m$  cell and given per formula unit) of the  $C2/m$ ,  $P2_1/c$  and  $P2/c$  cells as a function of  $U_{\text{eff}}$

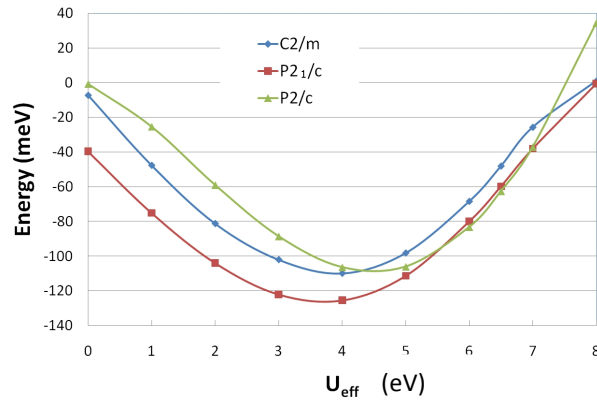
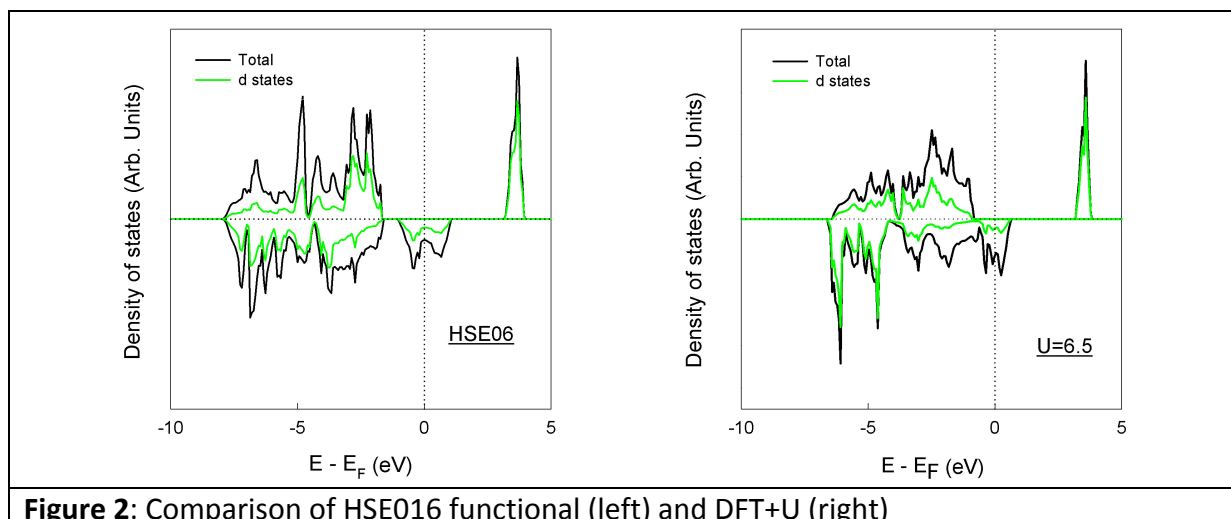


**TABLE II.** The optimised geometries of cells and calculated magnetic moments on nickel ions. Values in italics are from the screened hybrid functional HSE016. Experimental values are reported in brackets ( $R\bar{3}m$ <sup>38</sup>;  $C2/m$ <sup>5</sup>, the Ni-O bond lengths quoted here are taken from the analysis of the Rietveld refinement, not the neutron PDF analysis as discussed in the text below since this is not tied to the  $C2/m$  symmetry).

Space Group	a (Å)	b (Å)	c (Å)	$\beta$ (degrees)	$d_{\text{Ni-O}}$ (Å)	Magnetic moment ( $\mu_B$ )
$R\bar{3}m$	2.9023 2.8491 (2.8788)		14.1889 14.1938 (14.2035)		1.99[6] 1.95[6] (1.974)	1.419
$C2/m$	5.151 (4.9693)	2.7929 (2.8774)	5.1461 (4.9967)	112.011 (109.204)	1.90[4], 2.14[2] (1.94[4], 1.96[2])	1.108
$P2_1/c$	5.8468	2.9302	4.90974	125.641	1.91[4], 2.12[2]	1.140
$P2/c$	5.0291	5.8059	4.942	70.6822	Ni(a) 2.05-2.07 Ni(b) 1.88-1.91	Ni (a) 1.759 Ni (b) 0.128

The cell parameters of the  $R\bar{3}m$  cell are shown in Table II and demonstrate good agreement with the experimental values. Figure 1 shows the density of states of the  $R\bar{3}m$  cell. The empty spin-up  $e_g$  band and half empty spin-down  $e_g$  band indicates an electronic configuration  $t_{2g}^6 e_g^1$  which corresponds to the  $d^7$  state or  $\text{Ni}^{3+}$ .  $\text{LiNiO}_2$  is reported to be a semiconductor with a band gap of about 0.5eV<sup>39</sup> but in the cell the spin-down  $e_g$  band lies on the Fermi level which implies conducting behaviour. The symmetry of the  $R\bar{3}m$  cell ensures that all six Ni-O bonds are identical and disagrees with the observation of different Ni-O bond lengths seen in experiment<sup>5,8</sup>. We have also performed calculations using the screened hybrid functional HSE016<sup>40</sup> to compare with the DFT+U results.



This is shown in Figure 2. Both methods predict that  $\text{LiNiO}_2$  in this cell should be a metal because the half-filled  $e_g$  band includes the Fermi level. The main difference is the gap between the  $e_g$  band and the rest of the valence band states in the hybrid functional calculation. Both calculations show that the  $e_g$  states are a mixture of Ni and O character. They are not largely O character (as might be expected from the Hartree Fock calculations on Li-doped NiO briefly discussed above). Also, the results show that the DFT+U calculations give a reasonable picture of the behaviour of the system. For reasons of computational resources, it is not practical to perform full optimisations using the HSE06 functional for all the unit cells we consider.

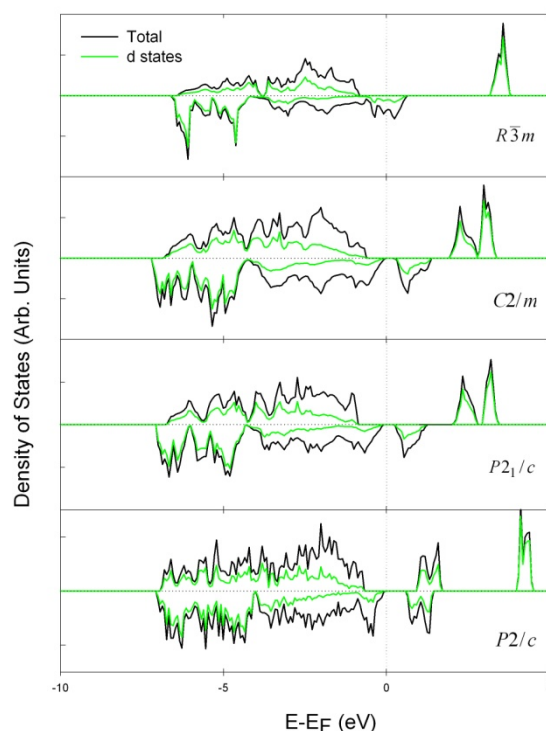


**Figure 3.** The density of states of the four candidate unit cells for  $\text{LiNiO}_2$ . Cells are indicated as above. Note that only the Jahn-Teller distorted ( $C2/m$ ,  $P2_1/c$ ) or charge disproportionating ( $P2/c$ ) cells show semi-conducting behaviour.

In the optimised  $C2/m$  cell, there are four short Ni-O bonds at 1.90 Å and two long Ni-O bonds at 2.14 Å which corresponds to a Jahn-Teller distorted system. These results are in good agreement with the previous work of [13] and [25] (quoted as the  $+Q_3$  mode). The total density of states of the  $C2/m$  cell shown in Figure 3 shows a split in the  $e_g$  band relating to a Jahn-Teller distortion. The band gap is approximately 0.5 eV, again in good agreement with the experimental data. Two unoccupied spin-up  $e_g$  states and one unoccupied spin-down  $e_g$  state are present which indicates an electronic configuration  $t_{2g}^6 e_g^1$ , or  $Ni^{3+}$ . This cell appears to be an accurate description for the Jahn-Teller relaxed structure generally accepted as the ground state of  $LiNiO_2$ . However, this cell presupposes a long-range cooperative Jahn Teller distortion which is not observed.

In the  $P2_1/c$  cell, all Ni ions are Jahn-Teller distorted with 4 short Ni-O and 2 long Ni-O bonds, implying the presence of  $Ni^{3+}$  ions. The geometrical difference from the  $C2/m$  cell is that the orientations of Jahn-Teller distortions in this cell are in a zigzag ordering. This induces, as expected<sup>5</sup>, significant distortion of the lattice from the  $C2/m$  cell which is not observed in experiment. The results are similar to previous work<sup>13</sup>; the most notable change being that the monoclinic angle found here ( $125^\circ$ ) is significantly larger than previously ( $107.87^\circ$ ). From Figure 3, the electronic structure of this  $P2_1/c$  cell is almost identical to the  $C2/m$  cell since the Ni ions are all  $Ni^{3+}$  in both cells. Nevertheless, it will be shown that this zigzag Jahn-Teller ordering is more stable than the collinear case. Calculations were also performed using the  $Pm$  cell (which represents a trimer ordering case) and coordinates of [12] as a starting point. Results without relaxation produced a cell of significantly higher energy (per formula unit) than the  $R\bar{3}m$  cell. The higher energy of this structure may be due to the geometrical frustration identified by [5] resulting in significant strain in the structure. We are not able to relieve this strain by introducing the large-scale curvature suggested in [5] – the number of atoms required for such a calculation are beyond what *ab initio* calculations can currently consider. Upon geometrical relaxation, the  $Pm$  cell relaxed to a cell of  $P2_1/c$  symmetry with the behaviour discussed above. The issue of trimer ordering is considered in much more detail in [13].

The  $P2/c$  cell contains four  $LiNiO_2$  formula units and two inequivalent Nickel sites in a zigzag ordering. The total density of states in Figure 1 indicates that the  $P2/c$  cell is a semiconductor with a band gap about 0.5 eV, in good agreement with the measured value. In the optimised geometry, Ni(a) has six long Ni-O bonds at 2.04 ~ 2.07 Å with a magnetic moment of 1.759  $\mu_B$ . The local density of states in Figure 4 shows that one  $e_g$  band is unoccupied (the spin-down band but the choice is arbitrary), indicating the (high-spin) electronic configuration  $t_{2g}^6 e_g^2$  or  $Ni^{2+}$ . Ni(b) has six short Ni-O bond lengths at 1.88 ~ 1.91 Å with a magnetic moments 0.128  $\mu_B$ . The local density of states in Figure 4 for Ni(b) shows that both the spin-up and spin-down  $e_g$  bands are unoccupied, indicating the electronic configuration  $t_{2g}^6 e_g^0$  or low-spin  $Ni^{4+}$ .



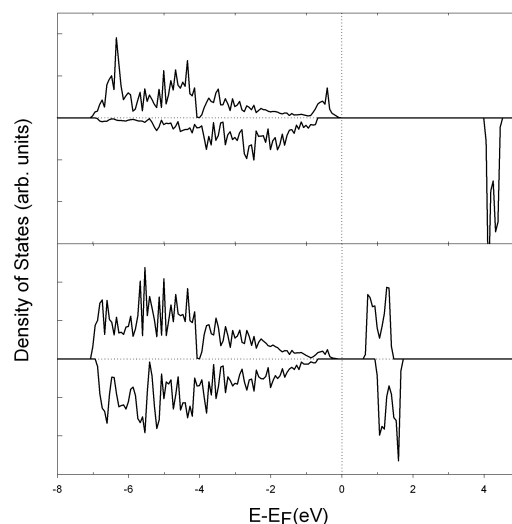


**Figure 4.** Local density of states for the two inequivalent nickels in the  $P2/c$  cell. The top diagram shows the nickel with six long Ni-O bonds. The bottom diagram shows the nickel with six short Ni-O bonds.

Figure 5 shows the iso-surface of the charge density difference which demonstrates substantially different amounts of electron density on the two Nickel ions. The  $P2/c$  cell therefore shows charge disproportionation. Although not reported in experiments, the  $P2/c$  cell reproduces the insulating character of  $\text{LiNiO}_2$  and the amount of monoclinic distortion displayed is about  $0.22^\circ$ , in very good agreement with the value  $0.16^\circ$  detected by neutron diffraction at low temperature<sup>9</sup> in the sample assigned to  $C2/m$  symmetry.

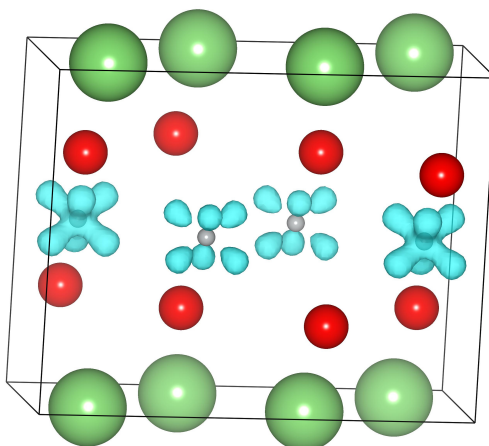


**Figure 5.** Charge density difference map for the  $P2/c$  cell. Green denotes Li, red denotes O, blue denotes Ni. Note the differences between the two kinds of Ni atom.

We emphasise that, despite our simple denotation of the nickel charge states as  $\text{Ni}^{3+}$  and  $\text{Ni}^{4+}$ , there is considerable charge transfer between the nickel and oxygen ions. This is clear from the densities of states in Figure 3 from looking at the amount of d character shown in

the figures. A similar point is made by the Mulliken and Bader charges shown in Table III below.

**TABLE III.** Mulliken and Bader charges of nickel and oxide ions in the cells calculated cells. The values in brackets are the volumes ( $\text{\AA}^3$ ) within which the charge is calculated.

Space Group	Mulliken charge (Ni)	Bader Charge (Ni)	Bader Charge (O)
$R\bar{3}m$	9.229	8.6329 (7.5376)	7.183
$C2/m$	9.335	8.5541 (7.1567)	7.223
$P2_1/c$	9.322	8.5741 (7.182)	7.213
$P2/c$	Ni (a) 9.098 Ni (b) 9.568	Ni(a) 8.721 (8.279) Ni(b) 8.515 (6.425)	O(a) 7.123 O(b) 7.259

The lattice energies of the four cells are listed in Table IV. The lowest energy cell for  $\text{LiNiO}_2$  is that with  $P2/c$  symmetry. This suggests that charge disproportionation must be considered as a reasonable mechanism to remove the orbital degeneracy of  $\text{Ni}^{3+}$  in  $\text{LiNiO}_2$ . The ordering of the other cells is the same as for previous work<sup>13</sup> but the relative stabilisation energies somewhat different – the ones quoted here are about twice those in [13]. This can reasonably be ascribed to the different  $U_{\text{eff}}$  values used. The lattice energy of the  $P2/c$  cell is, however, only about 2 meV lower than the  $P2_1/c$  cell (the equivalent of 25 K and well within the margin of error of the calculation) and 14.5 meV lower than the  $C2/m$  cell (the equivalent of 170 K and probably within the margin of error). Table 3 also shows the lattice energies for  $\text{NaNiO}_2$  in the three different symmetries explored for  $\text{LiNiO}_2$ .  $\text{NaNiO}_2$ , unlike  $\text{LiNiO}_2$ , is found exclusively in the Jahn-Teller relaxed state. Previous calculations<sup>41</sup> on the  $R\bar{3}m$  and  $C2/m$  cells of  $\text{NaNiO}_2$  were performed using a  $U_{\text{eff}}$  value of 4.5eV but from Figure 1 it is clear that similar results are expected for our value of 6.5eV except for the  $P2/c$  disproportionation cell which the previous work did not consider. Our calculations find the lowest energy configuration to be the cooperative  $C2/m$  Jahn-Teller cell by approximately 32meV (and 58meV below the charge-disproportionation cell  $P2/c$ ). This is many times the energy difference between the lowest-energy Jahn-Teller cell and the charge disproportionation cell in  $\text{LiNiO}_2$ .

**TABLE IV:** Calculated lattice energies per formula unit (meV) relative to the  $R\bar{3}m$  cell using a  $U_{\text{eff}}$  parameter of 6.5eV. The lowest energy cells are shown in bold. The Pm cell is shown in italics since it is unrelaxed.

	$\text{LiNiO}_2$	$\text{NaNiO}_2$
Pm (expt. cords. From [16])	<i>+61.80</i>	n/a
$R\bar{3}m$	0	0
$C2/m$	-48.05	<b>-78.65</b>
$P2_1/c$	-60.37	-46.28
$P2/c$	<b>-62.56</b>	-20.53

Our results suggest that both Jahn-Teller distortion and charge disproportionation are possible in samples of  $\text{LiNiO}_2$  at the temperatures at which all the experiments to determine the structure were performed. The EXAFS experiments<sup>8</sup> were performed at room temperature; no temperature is reported for the electron diffraction work<sup>12</sup> but it is reasonable to infer that it was performed at room temperature; the neutron diffraction was performed at a range of temperatures between 10 K and 585 K. This may explain the differences in reported experimental structures. Slight changes in the *growth* conditions, stoichiometry, and other variables could favour the formation of one cell rather than another. It is also possible that both relaxations can occur within the same sample within different grains for example or at the surface versus the bulk or there exists a more stable phase with a complicated charge-orbital ordering pattern, in which  $\text{Ni}^{2+}$ ,  $\text{Ni}^{3+}$  and  $\text{Ni}^{4+}$  coexist.

The  $P2/c$  cell matches the majority of the reported experimental findings, two different Ni-O bond lengths, the small monoclinic distortion, the band gap and the lack of Jahn-Teller related magnetic properties. Its most important failure is that such a cell should give an approximately 1:1 ratio of the Ni-O short to long bonds rather than the approximate ratio of 2:1 observed in [5] (assuming that we group the Ni—O bond lengths as suggested there). However, if the PDF in [5] is sampling a mixture of the cells involving charge disproportionation and Jahn-Teller distortion, then our results are consistent with this work since it is clear from the PDF that there is a range of Ni-O distances which contribute to the approximate 2:1 ratio depending on how they are grouped together. We would also have a natural explanation for the domain structure claimed by [9] at low temperatures.

We turn finally to the magnetic data. Both the data of ref [11] and the more recent  $\mu\text{SR}$  data<sup>42</sup> suggest that the ferromagnetic and antiferromagnetic states are close in energy. The ESR data suggests that the dominant interactions are ferromagnetic, but that strong antiferromagnetic fluctuations exist between 13 K and 50 K. However, the saturation of the linewidth suggests that the antiferromagnetic correlations do not propagate below 10 K. The detailed interpretation of the behaviour in terms of orbital frustration is not consistent with later neutron<sup>5</sup> and electron diffraction<sup>12</sup> work. The  $\mu\text{SR}$  data predicts different magnetic ground states for different compositions of  $\text{Li}_{1-x}\text{Ni}_x\text{O}_2$ ; ferromagnetic for  $x = 0.03$  and  $x = 0.15$ ; antiferromagnetic for  $x = 0.02$ . The authors state that this supports the idea that the change in magnetic state is a bulk effect rather than demonstrating the formation of ferromagnetic or antiferromagnetic domains.

Our calculations cannot fully resolve this issue because of the limited accuracy of density functional theory calculations, but they can illustrate why the complexity exists. We have performed spin-polarised calculations on all the unit cells considered above. The  $C2/m$  cell has a ferromagnetic ground state with ferromagnetic coupling both within the layers and between the layers, but a mixed state with ferromagnetic coupling within the layers but antiferromagnetic coupling between the layers is only 3 meV above it in energy. For the  $P2_1/c$  cell, the ferromagnetic ground state is again lowest, but an antiferromagnetic state is

only 5meV above it. A similar result is obtained for the  $P2/c$  cell (which is the one that shows disproportionation of  $Ni^{3+}$ ) but here, the antiferromagnetic state is only 3 meV above the ferromagnetic ground state. Although the figures apparently predict a ferromagnetic ground state two points should be noted. First, the density functional calculations are not accurate to a few meV. Second, 1meV (in terms of  $kT$ ) corresponds to about 11 K. The calculations are entirely consistent with the great magnetic complexity observed.

## Conclusions

We have calculated three different cells of  $LiNiO_2$  and predict a new ground state crystal structure with  $P2/c$  space group symmetry. In this cell, the charge disproportionation reaction  $2Ni^{3+} \rightarrow Ni^{2+} + Ni^{4+}$  occurs which gives two groups of Ni-O bond lengths and the experimentally observed semiconducting behaviour. As a result, the ground state valency of Ni ions should be half 2+ and half 4+ charge state. Also the  $P2/c$  cell is consistent with the slight monoclinic distortion found at low temperature (10 K). Therefore the absence of cooperative Jahn-Teller distortion is well justified by this cell. Nonetheless, since the energy difference between two mechanisms is extremely small, and we cannot exclude the possibility that a trimer ordered system, stabilised by local (but still mesoscale) curvature is important. Our results do exclude the possibility that a space group incorporating the trimer ordering (the  $Pm$  space group suggested by [12]) can be the ground state configuration. This supports the hypothesis that the mechanism by which individual nickel ions remove orbital degeneracy could easily be influenced by its local environment. This is probable since the various ways of ordering the Jahn-Teller distorted  $Ni^{3+}$  ions are all likely to involve significant strain effects caused by local distortion.

In real samples, due to thermal effect and impurities, both Jahn-Teller distortion and charge disproportionation may occur and the Nickel valency could be a mixture of 2+, 3+ and 4+.  $Ni^{4+}$  would be expected to show an unusually short Ni-O bond length. This is seen in some of charge-ordered nickelates (see Table 1) and occasionally elsewhere<sup>43</sup>.

Since  $Ni^{4+}$  has a very low magnetic moment, this provides an alternative method for relieving the magnetic frustration expected in this compound but our calculations are not accurate enough to predict the ground magnetic state of the system unambiguously.

Finally, we have illustrated the difference between  $LiNiO_2$  and  $NaNiO_2$ . In  $NaNiO_2$ , there is only one dominant mechanism which is Jahn-Teller distortion. Here it is comparably easy to determine its ground state crystal and electronic structure without any dispute. The different case of  $LiNiO_2$ , where a number of different possible ground states are very close in energy, illustrates how two systems which are apparently so similar chemically, can nevertheless have very different behaviour.

## Acknowledgements

We thank EPSRC for funding under Grant number - EP/G005001/1. Via our membership of the UK's HPC Materials Chemistry Consortium, which is funded by EPSRC (EP/F067496), this work made use of the facilities of HECToR, the UK's national high-performance computing service, which is provided by UoE HPCx Ltd at the University of Edinburgh, Cray Inc and NAG Ltd, and funded by the Office of Science and Technology through EPSRC's High End Computing Programme. We thank Keith Refson (STFC, Rutherford-Appleton Laboratory) for useful discussions on the calculations.

## References

- <sup>1</sup> D. Mertz, Y. Ksari, F. Celestini, J. M. Debierre, A. Stepanov, and C. Delmas, *Physical Review B* **61**, 1240 (2000).
- <sup>2</sup> L. A. Montoro, M. Abbate, E. C. Almeida, and J. M. Rosolen, *Chemical Physics Letters* **309**, 14 (1999).
- <sup>3</sup> J. S. Kang, S.S. Lee, G. Kim, H.J. Lee, H.K. Song, Y.J. Shin, S.W. Han, C. Hwang, M.C. Jung, H.J. Shin, B.H. Kim, S.K. Kwon and B.I. Min, *Physical Review B* **76**, 195122 (2007).
- <sup>4</sup> H. Ikeno, I. Tanaka, Y. Koyama, T. Mizoguchi, and K. Ogasawara, *Physical Review B* **72**, 075123 (2005).
- <sup>5</sup> J. H. Chung, Th. Proffen, S. Shamato, A.M. Ghorayeb, L. Croguennec, W. Tian, B.C. Sales, R. Jin, D. Mandrus and T. Egami *Physical Review B* **71**, 064410 (2005).
- <sup>6</sup> M. K. Aydinol, A. F. Kohan, G. Ceder, K. Cho, and J. Joannopoulos, *Physical Review B* **56**, 1354 (1997).
- <sup>7</sup> L. Petit, G. M. Stocks, T. Egami, Z. Szotek, and W. M. Temmerman, *Physical Review Letters* **97**, 146405 (2006).
- <sup>8</sup> A. Rougier, C. Delmas, and A. V. Chadwick, *Solid State Communications* **94**, 123 (1995).
- <sup>9</sup> I. Nakai, K. Takahashi, Y. Shiraishi, T. Nakagome, and F. Nishikawa, *Journal of Solid State Chemistry* **140**, 145 (1998).
- <sup>10</sup> J. B. Goodenough, D. G. Wickham, and W. J. Croft, *Journal of Physics and Chemistry of Solids* **5**, 107 (1958).
- <sup>11</sup> F. Reynaud, D. Mertz, F. Celestini, J. M. Debierre, A. M. Ghorayeb, P. Simon, A. Stepanov, J. Voiron, and C. Delmas, *Physical Review Letters* **86**, 3638 (2001).
- <sup>12</sup> J. Cao, H. Zou, C. Guo, Z. Chen, and S. Pu, *Solid State Ionics* **180**, 1209 (2009).
- <sup>13</sup> Z. Chen, H. Zou, X. Zhu, J. Zou and J. Cao, *J. Solid State Chem.* (2011) doi:10.1016/j.jssc.2011.05.024
- <sup>14</sup> J.L. Garcia-Munoz, J. Rodriguez-Carvajal, P. Lacorre, and J. B. Torrance, *Physical Review B* **46**, 4414 (1992).
- <sup>15</sup> J.L. Garcia-Munoz, M. A. G. Aranda, J. A. Alonso and M. J. Martinez-Lope, *Physical Review B* **79**, 134432 (2009).
- <sup>16</sup> J. A. Alonso, M.J. Martinez-Lope, M.T. Casais, J.L. Garcia-Munoz and M.T. Fernandez-Diaz, *Physical Review B* **61**, 1756 (2000).
- <sup>17</sup> J. A. Alonso, J.L. Garcia-Munoz, M.T. Fernandez-Diaz, M.A.G. Aranda, M.J. Martinez-Lope and M.T. Casais, *Physical Review Letters* **82**, 3871 (1999).
- <sup>18</sup> E. Wawrzynska, R. Coldea, E. M. Wheeler, T. Sorgel, M. Jansen, R. M. Ibberson, P. G. Radaelli, and M. M. Koza, *Physical Review B* **77**, 094439 (2008).
- <sup>19</sup> X. Yang, K. Takada, M. Itose, Y. Ebina, R. Ma, K. Fukuda, and T. Sasaki, *Chemistry of Materials* **20**, 479 (2007).

20 I. I. Mazin, D. I. Khomskii, R. Lengsdorf, J. A. Alonso, W. G. Marshall, R. M. Ibberson,  
A. Podlesnyak, M. J. Martinez-Lope, and M. M. Abd-Elmeguid Physical Review Letters **98**,  
176406 (2007).

21 W.C. Mackrodt, N.M. Harrison, V.R. Saunders, N.L. Allan and M.D. Towler, Chem. Phys. Lett.  
**250** 66 (1996)

22 W.C. Mackrodt and D.S. Middlemiss, J. Phys. Cond. Mat. **16** S2811 (2004)

23 P. Kuiper, G. Kruizinga, J. Ghijsen, G.A. Sawatsky and H. Verweij, Phys. Rev. Lett. **62** 221  
(1989)

24 M.K. Aydinol, A.F. Kohan, G. Ceder, K. Cho and J. Joannopoulos, Phys. Rev. B **56** 1354 (1997)

25 C. A. Marianetti, D. Morgan, and G. Ceder, Physical Review B **63**, 224304 (2001).

26 K. Mukai, J. Sugiyama and Y. Aoki, J. Solid State Chem. **183** 1726 (2010).

27 V.I. Anisimov, J. Zaanen and O.K. Andersen, Phys. Rev. B **44** 943 (1991)

28 J. P. Perdew, K. Burke, and M. Ernzerhof, Phys. Rev. Lett. **77**, 3865 (1996).

29 P. E. Blochl, Phys. Rev. B **50**, 17953 (1994).

30 S. K. Mishra and G. Ceder, Physical Review B **59**, 6120 (1999).

31 S. L. Dudarev, G. A. Botton, S. Y. Savrasov, C. J. Humphreys, and A. P. Sutton, Physical Review  
B **57**, 1505 (1998).

32 F. Zhou, M. Cococcioni, C. A. Marianetti, D. Morgan, and G. Ceder, Physical Review B **70**,  
235121 (2004). The reader should note that the values for  $U_{\text{eff}}$  given there (Table II) are  
6.7eV for  $\text{Ni}^{3+}$  and 6.04eV for  $\text{Ni}^{4+}$ . Our results show that there is no significant difference  
observed in changing the  $U_{\text{eff}}$  by a few tenths of an electron volt and we have chosen 6.5eV  
for convenience.

33 C. Y. Ouyang, S. Q. Shi, and M. S. Lei, Journal of Alloys and Compounds **474**, 370 (2009).

34 S. Yamamoto and T. Fujiwara, J. Phys. Soc. Jpn. **71**, 1226 (2002).

35 H.-T. Jeng, G. Y. Guo, and D. J. Huang, Physical Review Letters **93**, 156403 (2004).

36 F. Zhou and G. Ceder, Physical Review B **81**, 205113 (2010).

37 G. Kresse, and J. Furthmuller, Physical Review B **54**, 11169 (1996).

38 W.Li, J.N. Reimers and J.R. Dann, Solid State Ionics **67** 123 (1993).

39 J. Molenda, P. Wilk, and J. Marzec, Solid State Ionics **146**, 73 (2002).

40 A.V. Krukau, O.A. Vydrov, A.F. Izmaylov, and G.E. Scuseria, J. Chem. Phys. **125** 224106  
(2006).

41 H. Meskine and S. Satpathy, J Appl. Phys. **97** 10A314 (2005)

42 J. Sugiyama, Y. Ikedo, K. Mukai, H. Nozaki, M. Mansson, O. Ofer, M. Harada, K. Kamazawa,  
Y. Miyake, J.H. Brewer, E.J. Ansaldo, K.H. Chow, I. Watanabe and T. Ohzuku, Physical Review  
B **82**, 224412 (2010).

43 A. N. Mansour, L. Croguennec, and C. Delmas, Electrochem. Solid State Lett. **8**, A544 (2005).